Knapp, K. R. and L. L. Stowe, Deriving an aerosol optical depth climatology over land using AVHRR, presented at the *International Radiation Conference 2000*, St Petersburg, Russia, July 2000 … to printed in the IRS 2000 Proceedings.

DERIVING AN AEROSOL OPTICAL DEPTH CLIMATOLOGY OVER LAND USING AVHRR

Kenneth R. Knapp
CIRA –NOAA/NESDIS/ORA
Camp Springs, MD 20746, USA

Larry L. Stowe
NOAA/NESDIS, Office of Research and Applications
Camp Springs, MD 20746

ABSTRACT

Retrieval of aerosol optical depth (AOD) over land from satellite platforms has been limited in comparison to the number of retrievals over oceanic areas. Significantly, the NOAA Advanced Very High Resolution Radiometer (AVHRR) has provided nearly 20 years of AOD retrievals over the oceans with no corresponding retrieval over land. This retrieval gap is primarily due to uncertainties in the surface reflecting properties limiting retrieval performance. However, the length of AVHRR observations allows this variation to be deduced, leaving a residual which we hypothesize is an aerosol signal. First, the aerosol signal is estimated by removing surface and Rayleigh scattering effects. Then this proposed aerosol signal is compared to ground measurements of AOD. Results suggest that this aerosol signal is present and could be used to retrieve AOD over some land regions.

1. INTRODUCTION

With the reprocessing of AVHRR data back to 1981 by the AVHRR Pathfinder Atmosphere (PATMOS) project at NOAA/NESDIS (Jacobowitz, 1999), cloud-free radiance statistics exist for each day on a global 110 km grid for all five channels of AVHRR. Ocean grid cell data have been processed with the NOAA operational aerosol retrieval algorithm to create the most extensive record of aerosol optical depth ever compiled. However, as theoretical climate model studies indicate, the most significant concentrations and radiative effects of aerosols occur over land. To assist these climate studies, as well as the Global Aerosol Climatology Project, we are developing an AOD retrieval algorithm over land, comparable to the one over oceans where and when an aerosol signal is present in the 0.63 micron reflectance channel of AVHRR.

The first step of this research was to determine an aerosol signal in the PATMOS data. A signal was found, but it is strongly dependent on the surface bidirectional reflectance distribution function (BRDF). The research presented herein attempts to minimize this BRDF effect on the PATMOS cloud-free visible reflectances over land.

2. DATA

Two data sources are used in this study: the PATMOS data set is used for cloud-free TOA reflectance observations and the AERONET data are used for aerosol optical depths.

2.1 PATMOS-1 Data

The Advanced Very High Resolution Radiometer (AVHRR) has flown nearly continuously on numerous NOAA satellites since 1981. This vast amount of data is condensed into a useable format in the PATMOS data set. The volume of the Global Area Coverage (GAC) AVHRR data has been significantly reduced from terabytes to gigabytes by statistically decreasing the spatial resolution. The GAC data are binned into 110×110 km^2 equal area grid cells. For each grid cell, statistics are calculated for each AVHRR channel.

The PATMOS data set includes 71 parameters for each grid cell. 54 parameters are direct variables of AVHRR measurements. Four statistical categories are used for each channel: All pixels, clear sky, aerosol burden and cloudy. Statistics for each category (generally, the mean and standard deviation) and recorded for each channel. The parameter used in this study is the channel 1 cloud-free, deemed cloud-free by the CLAVR-1 algorithm (Stowe et al., 1999).

For this study, the PATMOS data from 1996 through 1998 are used to compare with AERONET observations of aerosol optical depth.

2.2 AERONET Data

The Aerosol Robotic Network (AERONET), supervised by Brent Holben of NASA, provides the ground truth validation for this research. AERONET is a

federation of sun photometers independently owned with centrally archived data, which can measure aerosol optical depth to an accuracy of ±0.02 (Holben et al., 1998). Data used in this study utilizes only those sites where the data have been cloud filtered as well as post-calibrated (i.e., level 2 data).

3. LUT CALCULATIONS

The calculation of the Look-Up Table (LUT) is performed using the radiative transfer model and surface BRDF model described in this section.

3.1 SHDOM Radiative Transfer Model

The Spherical Harmonics Discrete Ordinate Method (SHDOM) radiative transfer model (Evans, 1998) is used to produce theoretical TOA reflectances. TOA reflectances were calculated at 12 solar zenith angles, θ_1: 15°-70°, 15 satellite zenith angles, θ_2: 0°-70° and 25 azimuth angles, ϕ_1-ϕ_2: 0°-180°. Atmospheric effects were limited to Rayleigh scattering (with an optical depth of 0.0414). In future retrievals, gaseous absorption and aerosol extinction will be included.

3.2 Surface BRDF Model – Rahman et al., 1993

Privette et al. (1997) compare different BRDF models and conclude that the model described by Rahman et al. (1993) describe a multitude of surfaces with higher accuracy than other methods. Therefore, it was used in this research to model the surface, via:

$$\rho_s(\theta_1,\theta_2,\phi_1-\phi_2) = \rho\frac{\cos^{k-1}\theta_1\cos^{k-1}\theta_2}{(\cos\theta_1+\cos\theta_2)^{1-k}}\cdot \frac{1-\Theta^2}{\left[1+\Theta^2-2\Theta\cos(\pi-g)\right]^{3/2}}\left(1+\frac{1-\rho}{1+G}\right)$$

where:

$$\cos g = \cos\theta_1\cos\theta_2+\sin\theta_1\sin\theta_2\cos(\phi_1-\phi_2)$$
$$G = \sqrt{\tan^2\theta_1+\tan^2\theta_2-2\tan\theta_1\tan\theta_2\cos(\phi_1-\phi_2)}.$$

Here, the surface is described by three terms: the magnitude of the surface reflectance, ρ; the Henyey-Greenstein function parameter, Θ; and the level of anisotropy, k. For each viewing geometry in the LUT, 4800 BRDF calculations were performed with ρ: 0.001 to 0.15, Θ: -1 to 1, and k: 0.2 to 1. Each BRDF was used in an SHDOM run to calculate the TOA reflectance due to the surface BRDF and Rayleigh scattering for each of the 4500 possible geometries.

4. BRDF RETRIEVAL METHOD

The aerosol signal in TOA reflectances is convoluted with the surface BRDF. This section describes how that BRDF is retrieved.

4.1 Clear-Sky Reflectance Determination

Given that aerosols increase the TOA reflectance (in the absence of strong absorption), then the darkest observation at a given geometry will likely have the least aerosols. This clear-sky reflectance (no aerosol or cloud) is primarily affected by the underlying BRDF, Rayleigh scattering and gaseous absorption (for channel 1, variance in ozone can affect the transmittance and is not included here, but will be included in further research). Enough observations of the surface must be observed with relatively low aerosol amount to better characterize the surface reflectance. However, the surface reflectance can change during this time period, and is more likely to change with longer time periods. Thus, any retrieval of the surface BRDF must observe enough days to sample the BRDF with small aerosol loading, but not so many days that the surface changes. The number of days used for an individual BRDF estimate will be termed the composite time.

In this study, the composite time was allowed to vary, but did not exceed 60 days. A composite time was determined when six of the nine observation angles (one from each of the 9 days in NOAA's satellite coverage repeat cycle) had at least three cloud-free observation. So, the shortest composite time could be 24 days. This required at least three observations for most observation angles. Thus, through the comparison of reflectance for each angle, the relative amount of aerosol could be estimated and used to estimate weights used in the BRDF retrieval. Larger weights were given to darker observations and smaller weights to brighter observations.

4.2 BRDF Retrieval

The BRDF retrieval uses a simplistic LUT approach. A cost function is minimized, thus determining the BRDF, via:

$$\text{Cost}_j = \sum_i\left[\frac{\left(R_{obs,i}-R_{LUT,i,j}\right)}{\sigma_{R,i}}\cdot w_i\right]^2 + \text{Penalty}_{i,j}$$

where:

- subscript j represents the 4800 BRDFs
- subscript i represents each cloud free observation in the compilation time
- $R_{obs,i}$ is the cloud-free reflectance
- $R_{LUT,i,j}$ is the TOA reflectance for the j^{th} BRDF
- $\sigma_{R,i}$ is the standard deviation of the cloud-free reflectances in the PATMOS grid cell
- w_i is the weight assigned to the $R_{obs,i}$, and

$$\text{Penalty}_{i,j} = \begin{cases} 1 & R_{obs,i} < R_{LUT,i,j} \\ 0 & R_{obs,i} \geq R_{LUT,i,j} \end{cases}$$

The penalty function is assigned because observed reflectances should rarely be less than a pure Rayleigh atmosphere, except due to noise. Thus the BRDF with the smallest cost function is the retrieved BRDF.

An example of a retrieval is shown in figure 1. The circles denote 26 days of cloud-free reflectances observed over Concepcion. The solid line represents the best BRDF fit ($\rho = 0.022$, $k = 0.52$, and $\Theta = 0.05$). The shading of the circles represents the weights given to each observation, based on the reflectances near it.

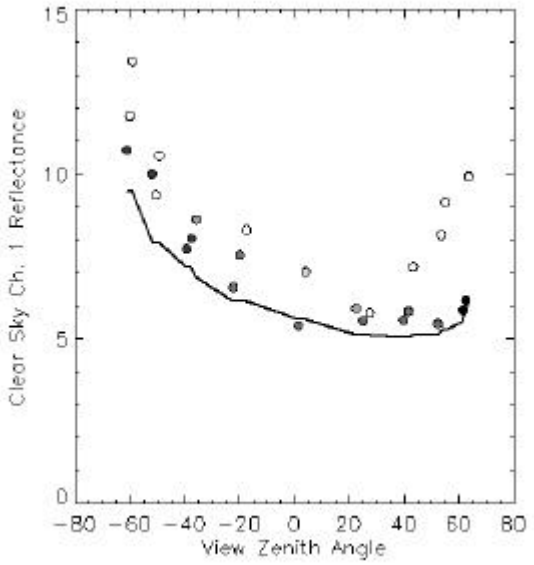

Figure 1 – Example fit of PATMOS cloud-free observations (circles) to a BRDF (solid line), the darker the shading, the more relative weight each observation received.

4. UNCERTAINTIES

Before discussing results, the uncertainty in these comparisons should be considered. Perhaps the most significant is the comparison of the once-daily satellite data to the nearly continuous ground measurements. The AERONET instrument field-of-view is on the order of meters, compared to the $110 \times 110 km^2$ spatial resolution of the PATMOS data. Also, the PATMOS observations are once per day, generally at the same time each day. The AERONET observations can be anytime during the day. Other uncertainties include changes in the surface and solar zenith angle during the composite time, variation in aerosol optical properties through the year and possible cloud contamination in the PATMOS cloud-free reflectances.

5. RESULTS

The BRDF retrieval is applied to over-land PATMOS grid cells where corresponding AERONET sites exist. This results in 37 comparison sites. An example of a comparison is shown in figure 2 for the Concepcion AERONET site in South America. First, un-corrected cloud-free reflectances are compared to AOD (diamonds). The correlation coefficient is 0.62, suggesting a signal in the data. Next, the reflectance deviation from the BRDF fit is compared to AOD (squares in figure 2). The corresponding correlation coefficient is 0.78 suggesting a significant increase in the amount of variance explained (from 38 to 60%). A summary of the correlation coefficients is given in Table 1. It can be seen that 33 of the 37 comparisons were positively correlated with AOD. The BRDF correction increased the correlation at ten of these sites and having negligible change for 18 others.

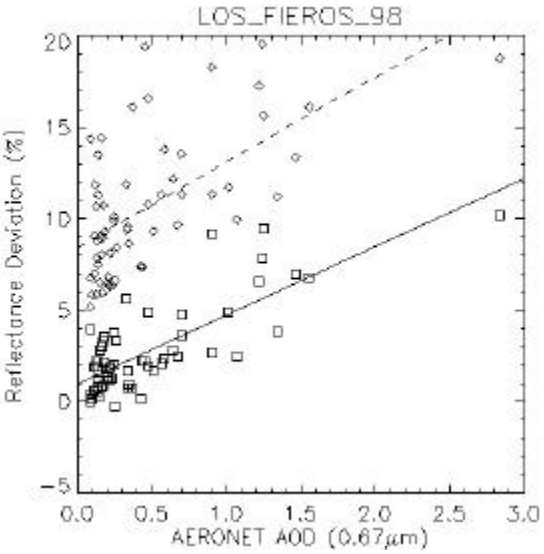

Figure 2 – Comparison of PATMOS cloud-free reflectances with AERONET AOD (diamonds) with linear regression line (dashed): $\rho = 4.64\tau + 8.45$, $r = 0.617$, $\chi^2 = 8.99$. Also, the deviation of cloud-free reflectance from the BRDF fit (square): $\rho = 3.74\tau + 0.97$, $r = 0.776$, $\chi^2 = 2.37$.

Perhaps more significant are the results of a simulated retrieval. The linear regression relationship before correction (from figure 2):

$$\rho = 4.64\tau + 8.45$$

can be inverted to simulate a simplistic retrieval:

$$\tau = \frac{\rho - 8.45}{4.64}$$

whose error is:

$$d\tau = \frac{d\rho}{4.64} \sim \frac{\sqrt{\chi^2}}{4.64} \sim 0.65.$$

where $\sqrt{\chi^2}$ is the standard error of estimate. This represents a simplistic noise estimate for the retrieval of AOD from the PATMOS data. The corresponding error estimate after BRDF correction is $d\tau = 0.41$. Suggesting a decrease in the noise of the relationship. A summary of the results at 37 sites is provided in Table 3. Of the 33 positively correlated sites, nearly half (15) have an 0.2 decrease in $d\tau$, with only seven sites having a significant increase in noise.

5. CONCLUSIONS

The surface BRDF is retrieved from PATMOS channel 1 cloud-free reflectance data and used to enhance the aerosol signal. Comparisons of aerosol signal (i.e., deviation of cloud-free reflectances from the BRDF fit) to AERONET AOD show less noise and higher correlation coefficients than uncorrected PATMOS cloud-free reflectances. Given the large number of uncertainties in this comparison and relatively short time period (3 years), these results suggest the possibility of retrieving aerosol optical depth from PATMOS data over a longer time period (i.e., 1981 to present).

Future research will extend these comparisons to other time periods and datasets. In addition to the AERONET dataset, the Multi-Filter Rotating Shadowband Radiometer (MFRSR) AOD dataset, Polarization and Directionality of the Earth's Radiance (POLDER) AOD and Total Ozone Mapping Spectrometer (TOMS) aerosol index could expand these comparisons to more regions than currently shown. It would also extend the comparisons to most of the 1990's and possibly the past two decades.

Table 1 - Table of correlation coefficients for before and after BRDF correction.

Condition	Number
All sites:	37
$r_{before} > 0.$	33
$r_{after} > 0.$	33
For $r_{after} > 0$:	
$r_{after} - r_{before} > 0.1$	10
$-0.1 < r_{after} - r_{before} < 0.1$	18
$-0.1 > r_{after} - r_{before}$	5

Table 2 - Table of simulated errors for before and after BRDF correction.

Condition	Number
All sites	37
$d\tau_{before} > 0.$	33
$d\tau_{after} > 0.$	33
For $d\tau_{after} > 0$:	
$d\tau_{before} - d\tau_{after} > 0.2$	15
$-0.2 < d\tau_{before} - d\tau_{after} < 0.2$	11
$-0.2 > d\tau_{before} - d\tau_{after}$	7

ACKNOWLEDGMENTS

This work is supported by the NASA/Global Aerosol Climatology Project (GACP). We acknowledge Brent Holben of NASA and the Principle Investigators of each AERONET site for the use of their data, which is available at http://aeronet.gsfc.nasa.gov:8080/.

REFERENCES

Evans, K. F., 1998: The Spherical Harmonics Discrete Ordinate Method for Three-Dimensional Atmospheric Radiative Transfer, J. Atmos. Sci., 55, 429-446.

Holben, B. N. et al., 1998: AERONET – A Federated Instrument Network and Data Archive for Aerosol Characterization, Remote Sens. Environ., 66, 1-16.

Jacobowitz, H.: AVHRR PATMOS datasets Available Online from NOAA, Bull. Amer. Meteor. Soc., 80, 967-968.

Privette, J. L., T. F. Eck and D. W. Deering, 1997: Estimating spectral albedo and nadir reflectance through inversion of simple BRDF models with AVHRR/MODIS-like data, J. Geophys. Res., 102, 29529-29542.

Rahman, H., B. Pinty and M. M. Verstraete, 1993: Coupled Surface-Atmosphere Reflectance Model 2. Semiempirical Surface Model Usable with NOAA Advanced Very High Resolution Radiometer Data, J. Geophys. Res., 98, 20791-20801.

Stowe, L. L., P. A. Davis and E. P. McClain, 1999: Scientific Basis and Initial Evaluation of the CLAVR-1 Global Clear/Cloud Classification Algorithm for the Advanced Very High Resolution Radiometer, J. Atm. Oceanic Tech., 16, 656-681.